Jour. Korean Earth Science Society, v. 28, no. 7, p. 936–946, December 2007

Geopotential Field in Nonlinear Balance with the Sectoral Mode of Rossby-Haurwitz Wave on the Inclined Rotation Axis

Hyeong-Bin Cheong* and Ja-Rin Park

Department of Environmental Atmospheric Sciences, Pukyong National University, 599-1 Daeyeon-3-dong, Namgu, Busan 608-737, Korea

섹터모드의 로스비하우어비츠 파동과 균형을 이루는 고도장

정형빈* · 박자린

부경대학교 환경대기과학과, 608-737 부산시 남구 대연 3동 599-1

Abstracts: Analytical geopotential field in balance with the sectoral mode (the first symmetric mode with respect to the equator) of the Rossby-Haurwitz wave on the inclined rotation axis was derived in presence of superrotation background flow. The balanced field was obtained by inverting the divergence equation with the time derivative being zero. The inversion consists of two steps, i.e., the evaluation of nonlinear forcing terms and the finding of analytical solutions based on the Poisson's equation. In the second step, the forcing terms in the form of Legendre function were readily inverted due to the fact that Legendre function is the eigenfunction of the spherical Laplacian operator, while other terms were solved either by introducing a trial function or by integrating the Legendre equation. The balanced field was found to be expressed with six zonal wavenumber components, and shown to be of asymmetric structure about the equator. In association with asymmetricity, the advantageous point of the balanced field as a validation method for the numerical model was addressed. In special cases where the strength of the background flow is a half of or exactly the same as the rotation rate of the Earth, it was revealed that one of the zonal wavenumber components vanishes. The analytical balanced field was compared with the geopotential field which was obtained using a spherical harmonics spectral model. It was found that the normalized difference lied in the order of machine rounding, indicating the reliability of the analytical results. The stability of the sectoral mode of Rossby-Haurwitz wave and the associated balanced field was discussed, comparing with the first antisymmetric mode.

Keywords: Rossby-Haurwitz wave, nonlinear balance equation, balanced geopotential, spectral method, Legendre function

요 약: 기울어진 자전축을 갖는 회전계에서, 일정한 각속도로 회전하는 동서풍이 있는 경우에 대해서 로스비하우어비츠 파동의 섹터모드(적도에 대한 반구 비대칭의 첫 번째 모드)와 균형을 이루는 지위고도장을 해석적으로 유도하였다. 균형장은 발산방정식으로부터 시간변화를 제거하고 라플라시안 연산자를 역산함으로써 구하였다. 역산은 비선형항의 계산과 포이슨 방정식의 해를 구하는 두 단계의 연산과정으로 이루어져 있다. 두 번째 단계에서, 구면조화함수로 표현되는 강제력의 항은 구면조화함수의 선형관계를 이용하였고, 그 이외의 항은 구면조화함수를 적분함으로써 구하였다. 균형장은 여섯 개의 동서파수 성분으로 표현됨이 드러났다. 본 연구에서 구한 균형장은 적도에 대하여 비대칭의 구조를 가지기 때문에, 대칭의 구조만을 가지는 것에 비하여 미분방정식의 수치해의 검증법으로서의 활용도가 높다. 일정한 각속도를 갖는 배경 동서풍이 지구의 자전각속도와 같거나 1/2에 해당하는 경우에는, 일부 동서파수 성분이 제거되는 것으로 나타났다. 이론적으로 구한 균형장은 정교한 수치모델을 통하여 구한 균형장과 거의 정확하게 같은 것으로 밝혀져, 이론적 해의 타당성이 입증되었다. 마지막으로, 로스비하우어비츠 파동의 섹터모드와 균형을 이루는 지위고도장의 안정성을 장기간시간적분을 통하여 살펴보았다.

주요어: 로스비하우어비츠 파동, 비선형 균형 방정식, 균형 고도장, 스펙트럴법, 르장드르 함수

*Corresponding author: hbcheong@pknu.ac.kr
Tel: 82-51-620-6286
Fax: 82-51-620-6286

Introduction

Large-scale atmospheric motions are known to be in geostrophic balance with the pressure or with geopotential field over global domain in good approximations except over the equatorial area. The geostrophic balance for the synoptic or long time-scale disturbances is better than that for the disturbances with short time scale. As the atmospheric disturbances are composed of global normal-mode waves, each normal-mode wave should be in good geostrophic balance. The global-scale flow (or geopotential) in geostrophic balance can be achieved by solving the global linear balance equation on the sphere (Daley, 1983). The poor balance over the equatorial belt in the case of geostrophic regime can be improved, if we use the nonlinear balance equation over the sphere. Although the geostrophic balance in this case does not hold in rigorous way, even off the equator, the balance between the mass and wind is improved in the context of barotropic motion (Daley, 1983; Swarztrauber, 1996; Ortland, 2005).

The normal mode of the nonlinear non-divergent barotropic motion is called Rossby-Haurwitz (R-H) wave, which is the Rossby wave defined on the global domain (Haurwitz, 1940). The R-H wave is expressed with the Legendre function in meridional direction and the Fourier harmonics in the zonal direction. Since the lower R-H mode for each zonal wavenumber is given as a simple function of the cosine latitude, it is of particular importance in many analytical approaches for numerical models. For example, the balanced field associated with the first antisymmetric mode has been used as a validation method for the numerical models for shallow water equations and primitive equations (Phillips, 1959; Williamson and Browning, 1973; Browning et al., 1989; Williamson et al., 1992; Cheong, 2006). The balanced geopotential field obtained by Phillips (1959) is now considered as a standard validation method, because it is provided with an analytical form. As illustrated in the literatures, the geopotential associated with the antisymmetric mode has a symmetric structure about the equator. To incorporate an asymmetric balance field is considered to be a more useful way in validating the numerical model because both symmetric and anti-symmetric structure are included.

For a given super-rotating background flow, the R-H waves of the same degree (or the total wavenumber-like index on the spherical surface) are the normal modes of the nondivergent barotropic equation (or the Legendre function), regardless of the zonal wavenumber. This implies that as the degree of the normal mode becomes large the number of R-H waves which can be considered as the normal mode increases. If we remember that the degree of the Legendre function remains the same even though it (or the R-H wave) is inclined about a coordinate axis, it can be said that a rotated Legendre function or the R-H wave is a normal mode of the nondivergent barotropic equation. In analytical approach, however, the procedure to obtain the balanced field for the inclined R-H wave is quite complicated due to the nonlinear terms associated with the inclination. The inclined R-H wave is very useful in validating a numerical model because it actually contains more-than-one zonal wavenumber components, unlike the other methods with analytical solutions (e.g., Läuter et al., 2005): The number of the zonal wavenumber components increases as the inclination angle approaches $\pi/2$.

In this study, the geopotential in balance with the sectoral mode of the R-H wave on an inclined rotation axis is obtained analytically. The divergence equation is used instead of the momentum equation, which was previously used by Phillips (1959) and Williamson et al. (1992) to avoid the complexities arising from the time derivative. An efficient way to invert the nonlinear balance equation will be presented in detail. In order to assess the reliability of the analytic geopotential field, a state-of-the-art numerical model is used.

This paper is organized as follows. In the next section, the R-H wave on the inclined rotation axis is given. The procedure to obtain the balanced geopotential associated with the R-H wave is presented in section 3. In section 4 the analytical geopotential field is

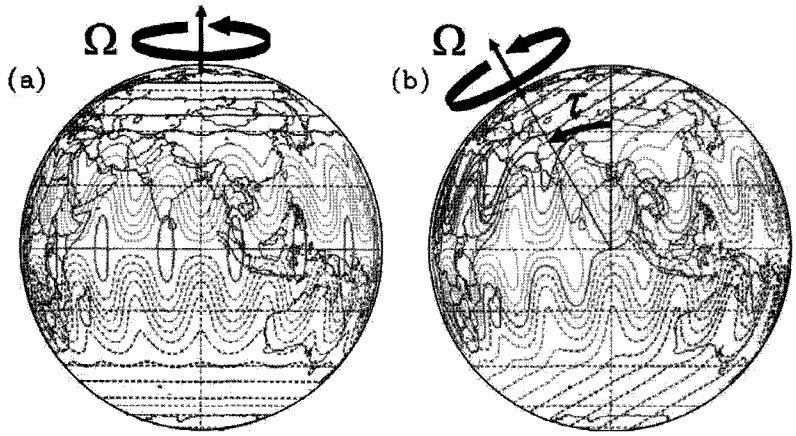

Fig. 1. Schematic illustration of the inclination of the rotation axis: The arrow denotes the rotation axis, and Ω means the rotation vector. (a) The rotating coordinate system without inclination, (b) The case of the inclination with $\tau = \pi/6$. For better illustration, a Rossby-Haurwitz wave of the first antisymmetric mode with zonal wavenumber 8, superimposed on the superrotating background flow, is plotted with orthographic map projection.

compared with that obtained numerically, and its stability is discussed. Summary and conclusions are given in the final section.

Rossby-Haurwitz Waves on the Inclined Rotation Axis

The Coriolis parameter f on the rotating coordinate system where the axis of rotation is inclined about y-axis toward South pole by the angle τ (see Fig. 1) is given as

$$f = 2\Omega(\cos\tau\sin\theta + \sin\tau\cos\lambda\cos\theta), \tag{1}$$

where λ and θ are the longitude and latitude, respectively, and Ω represents the rotation rate of the system. When the background flow is given to rotate around the inclined rotation axis, the R-H wave becomes a normal mode of the nonlinear vorticity equation. Let's consider the R-H wave of the first symmetric mode with the zonal wavenumber m in the presence of the basic flow:

$$\psi = -a^2\Omega(\omega\cos\tau\sin\theta + \omega\sin\tau\cos\lambda\cos\theta) + a^2K\Omega\cos^m\theta\cos m(\lambda - \sigma t), \tag{2}$$

where t, a, and Ω are the time, radius, and the inverse rotation rate (Ω^{-1}) of the Earth, respectively, ω is the strength of superrotation, σ is the angular velocity, K is the amplitude. Hereafter, for convenience, the dependent variables are nondimensionalized using a and Ω^{-1} as the length and time scale, respectively. The velocity components and relative vorticity associated with the R-H wave are written in nondimensional form as

$$\begin{aligned} u &= \omega\cos\tau\cos\theta - \omega\sin\tau\sin\theta\cos\lambda + m\cos^{m-1}\theta\sin\theta\cos m\lambda \\ v &= \omega\sin\tau\sin\lambda - Km\cos^{m-1}\theta\sin m\lambda \\ \zeta &= 2(\omega\cos\tau\sin\theta + \omega\sin\tau\sin\theta\cos\lambda) - Km(m+1)\cos^m\theta\cos m\lambda, \end{aligned} \tag{3a-c}$$

where $\zeta[\equiv\nabla^2\psi]$ with $\nabla^2 = \frac{1}{\cos^2\theta}\left(\frac{\partial^2}{\partial\lambda^2} + \cos\theta\frac{\partial}{\partial\theta}\cos\theta\frac{\partial}{\partial\theta}\right)$ was used.

Geopotential in Balance with the Rossby-Haurwitz Wave on the Inclined Rotation Axis

In this section, the balanced field associated with the R-H wave will be derived based on the nonlinear balance equation on the sphere. To obtain the geopotential field from the balance equation, the spherical Laplacian operator should be inverted with an appropriate method. The advantage of this method

(i.e., inversion method) over the traditional method which uses the momentum equations (e.g., Phillips, 1959; Williamson et al., 1992; Cheong, 2006) is that the difficulty related with time derivative term can be avoided. In general case where an arbitrary streamfunction field is given, the inversion can not be carried out analytically. The nonlinear balance equation, which corresponds to the divergence equation without the time derivative term, is written in dimensionless form as follows:

$$\nabla^2\left[\Phi+\frac{u^2+v^2}{2}\right]=G$$

$$G=\frac{1}{\cos^2\theta}\left[\frac{\partial}{\partial\lambda}V(\zeta+f)-\cos\theta\frac{\partial}{\partial\theta}U(\zeta+f)\right], \qquad (4)$$

where Φ is the geopotential, and $(U,V)\equiv(u,v)\cos\theta$ with u and v being the velocity components in longitudinal and latitudinal directions, respectively. Eq. (4) is a standard Poisson's equation in spherical coordinate system. The forcing function G can be evaluated with the use of vorticity and velocities given in (3). Once the forcing function is obtained, the geopotential is given by

$$\Phi=\nabla^{-2}G-\frac{u^2+v^2}{2}+\Phi_0, \qquad (5)$$

where ∇^{-2} denotes the inverse Laplacian operator and Φ_0 is a constant or the global average.

Since the balance equation is inherently nonlinear, the balanced geopotential will be composed of zonal wavenumber components whose number is larger than two, where the two refers to the zonal wavenumber m and 1 components which are associated with the R-H wave and the inclined rotation axis, respectively. Detailed procedure to get the balanced field is given below

The nonlinear terms consist of two terms. Substituting (3) into the advection terms yields

$$\begin{aligned}G=&-\omega(1+\omega)(2\cos^2\tau-\sin^2\tau)(3\cos^2\theta-2)\\&+\frac{1}{2}K^2m^2(m+1)\cos^{2(m-1)}\theta[(2m+1)\cos^2\theta-2m]\\&+12\omega(1+\omega)\cos\tau\sin\tau\cos\theta\sin\theta\cos\lambda\\&+3\omega(1+\omega)\sin^2\tau\cos^2\theta\cos2\lambda\\&+KmR\sin\tau\cos^{m-1}\theta\cos(m-1)\lambda\\&-Km[\omega(m+1)+2(1+\omega)(m+2)\cos\tau\cos^m\theta\sin\theta\cos m\lambda\\&-Km(m+2)\left[1+\omega+\frac{1}{2}\omega(m+1)\right]\sin\tau\cos^{m+1}\theta\cos(m+1)\lambda\\&+\frac{1}{2}K^2m^2(m+1)(2m+1)\cos^{2m}\theta\cos2m\lambda,\end{aligned} \qquad (6)$$

where

$$\begin{aligned}R=&\omega m^2+\omega m+2\omega+2+\\&\left(-\frac{1}{2}\omega m^2-\frac{5}{2}\omega m-3\omega-m-2\right)\cos^2\theta.\end{aligned} \qquad (7)$$

Note that the terms in equation (6) consist of terms that have the same order with respect to the cosine latitude except the terms related with the zonal wavenumber component $m+1$ and zero. The $m+1$ component contains two terms, each having the order of $\cos^{m-1}\theta$ and $\cos^{m+1}\theta$, while zero component contains $\cos^{k-1}\theta$ and $\cos^{k+1}\theta$ with $k=1$ in the first term and $\cos^{2(k-1)}\theta$ and $\cos^{2(k+1)}\theta$ with $k=m$ in the second term. The terms except the zonal wavenumber $m+1$ can be readily inverted because they are in the form of either Legendre function or simple function of cosine latitude. We have found that the method used in the previous studies (Phillips, 1959; Williamson et al., 1992; Cheong, 2006) is not appropriate for the case of inclination of the rotation axis. The functions of cosine or sine latitude included in (6) can be classified into one of the following forms:

$$\begin{aligned}&\cos^m\theta\cos m\lambda\\&\cos^m\theta\sin\theta\cos m\lambda\\&\cos^{2m-2}\theta[(2m+1)\cos^2\theta-2m]\\&(p\cos^{m-1}\theta+q\cos^{m+1}\theta)\cos(m-1)\lambda,\end{aligned} \qquad (8a\text{-}d)$$

where p and q are constants. Functions of (8a) and (8b) are inverted with ease because they are the Legendre functions:

$$\nabla^{-2}\cos^m\theta\cos m\lambda=-\frac{1}{m(m+1)}\cos^m\theta\cos m\lambda$$

$$\nabla^{-2}\cos^m\theta\sin\theta\cos m\lambda=-\frac{1}{m(m+1)(m+2)}\cos^m\theta\sin\theta\cos m\lambda, \qquad (9a,b)$$

Inverse Laplacian of (8c) can be obtained either by integrating the Laplacian operator with respect to the latitude, or by seeking the function in the form of $\cos^m\theta$ through trial and error. We have found that operation of the Laplacian to $\cos^m\theta$ results in (8c) with constant multiple of $(-2m)$, therefore,

$$\nabla^{-2}\cos^{2m-2}\theta[(2m+1)\cos^2\theta-2m]=\frac{1}{2}\cos^{2m}\theta. \quad (10)$$

Inversion of (8d) is performed by assuming that the inverse Laplacian (denoted as X) is composed of two terms, each having different order, e.g.,

$$X=(r\cos^{m-1}\theta+s\cos^{m+1}\theta)\cos(m-1)\lambda, \quad (11)$$

where r and s are constants. Applying the Laplacian operator to (11) and comparing the result with (8d), the constants r and s are determined:

$$\nabla^2(r\cos^{m-1}\theta+s\cos^{m+1}\theta)\cos(m-1)\lambda=$$
$$[\{4sm-rm(m-1)\}\cos^{m-1}\theta-s(m+1)(m+2)\cos^{m+1}\theta]$$
$$\cos(m-1)\lambda, \quad (12)$$

which yields

$$s=-\frac{q}{(m+1)(m+2)}$$
$$r=-\frac{p-4sm}{m(m-1)}. \quad (13)$$

In (13) r becomes infinite in case of $m=1$, which will make the balanced field singular. Fortunately, however, this does not happen because the factor $(m-1)$ disappears when the inverse Laplacian of G is combined with the kinetic energy term.

Then, the inverse Laplacian of the nonlinear terms has the form:

$$\nabla^{-2}G=\frac{1}{2}\omega(1+\omega)(2\cos^2\tau-\sin^2\tau)\cos^2\theta$$
$$-\frac{1}{4}K^2m(m+1)\cos^{2m}\theta$$
$$-2\omega(1+\omega)\cos\tau\sin\tau\cos\theta\sin\theta\cos\lambda$$
$$-\frac{1}{2}\omega(1+\omega)\sin^2\tau\cos^2\theta\cos2\lambda$$
$$+(R_1\cos^{m-1}\theta+R_2\cos^{m+1}\theta)K\sin\tau\cos(m-1)\lambda$$
$$+Km\left[\omega+\omega+\frac{2(1+\omega)}{m+1}\cos\tau\cos^m\theta\sin\theta\cos m\lambda\right.$$
$$\left.+Km\left[\frac{1}{2}\omega+\frac{(1+\omega)}{m+1}\right]\sin\tau\cos^{m+1}\theta\cos(m+1)\lambda\right.$$
$$-\frac{1}{4}K^2m(m+1)\cos^{2m}\theta\cos2m\lambda, \quad (14)$$

where

$$R_1=\frac{2m[\omega(m+3)+2]-[\omega m(m+1)+2(1+\omega)](m+1)}{(m-1)(m+1)}$$
$$R_2=\frac{m[\omega(m+3)+2]}{2(m+1)}. \quad (15)$$

Evaluation of the term representing the kinetic energy is straightforward. As in the case of the advection terms, there appear six non-zonal wavenumber components along with the zonal-mean component:

$$-\frac{u^2+v^2}{2}=-\frac{1}{2}\omega^2C_\tau^2C_\theta^2-\frac{1}{4}\omega^2S_\tau^2(1+S_\theta^2)$$
$$-\frac{1}{4}K^2m^2C_\theta^{2(m-1)}(1+S_\theta^2)+\omega^2S_\tau C_\tau C_\theta S_\theta\cos\lambda$$
$$+\frac{1}{4}\omega^2S_\tau^2C_\theta^2\cos2\lambda+\frac{1}{2}Km\omega S_\tau C_\theta^{m-1}(1+S_\theta^2)\cos(m-1)\lambda$$
$$-Km\omega C_\tau C_\theta^mS_\theta\cos m\lambda-\frac{1}{2}Km\omega S_\tau C_\theta^{m+1}\cos(m+1)\lambda$$
$$+\frac{1}{4}K^2m^2C_\theta^{2m}\cos2m\lambda, \quad (16)$$

where $C_\tau=\cos\tau$, $S_\tau=\sin\tau$, $C_\theta=\cos\theta$, and $S_\theta=\sin\theta$.

The balanced field, then, can be obtained by combining (14) and (16). After some manipulation of the coefficients for each zonal wavenumber components, we have

$$\Phi=\Phi_0+\frac{1}{4}\omega(2+\omega)(2C_\tau^2-S_\tau^2)C_\theta^2$$
$$-\frac{1}{4}K^2mC_\theta^{2(m-1)}(2m+C_\theta^2)$$
$$-\omega(2+\omega)C_\tau S_\tau C_\theta S_\theta\cos\lambda$$
$$-\frac{1}{4}\omega(2+\omega)S_\tau^2C_\theta^2\cos2\lambda$$
$$+K\frac{(1+\omega)}{(m+1)}[2+mC_\theta^2]S_\tau C_\theta^{m-1}\cos(m-1)\lambda$$
$$+Km\omega C_\tau C_\theta^mS_\theta\cos m\lambda-\frac{1}{2}Km\omega S_\tau C_\theta^{m+1}\cos(m+1)\lambda$$
$$-\frac{1}{4}K^2m^2C_\theta^{2m}\cos2m\lambda. \quad (17)$$

It is worthy to note that the singularity for the term related with $\cos(m-1)\lambda$, shown in Eq. (13), has disappeared. In Eq. (17) the highest order for the cosine latitude is $2m$, which corresponds to the twice of the total wavenumber of the streamfunction. There are only two terms which are independent of the wave amplitude of the streamfunction K: the zonal wavenumber component of one and two. These terms disappear in a special case of $\omega=-2$, i.e., easterly superrotation with the magnitude being the same as the Earth's rotation. In a special case where the inclination of the rotation axis is not considered, the geopotential field in (17) becomes

$$\Phi_{(\tau=0)} = \Phi_0 + \frac{1}{2}\omega(2+\omega)C_\tau^2 C_\theta^2 - \frac{1}{4}K^2 m^2 C_\theta^{2(m-1)}(2m+C_\theta^2) + Km\frac{2(1+\omega)}{(m+1)}C_\tau C_\theta^m S_\theta \cos m\lambda - \frac{1}{4}K^2 m C_\theta^{2m}\cos 2m\lambda . \quad (18)$$

In comparison with the first antisymmetric mode (Phillips, 1959; Williamson et al., 1992), the balanced field for the first symmetric mode has lower order by two for both the zonal-mean and wave components. It is easy to find that the geopotential field in (18) is asymmetric about the equator, due to the term related with $\cos m\lambda$.

Comparison with the Numerical Result and Stability

In this section, the analytical balanced field associated with the R-H wave will be compared with the balanced field which is obtained numerically. For this purpose, we use the spherical harmonics pseudo-spectral model (Orszag, 1970; Swarztrauber, 1996; Cheong, 2006). The dependent variables are expanded with the surface spherical harmonics function, which consists of the Legendre function and Fourier series in latitudinal and longitudinal directions, respectively, e.g.,

$$\zeta(\lambda,\theta) = \mathrm{Re}\left[\sum_{n=|m|}^{M}\sum_{m=-M}^{M}\zeta_{n,m}P_n^m(\mu)\exp im\lambda\right], \quad (19)$$

where $P_n^m(\mu)$ is the Legendre function of order m and degree n with $\mu\equiv\sin\theta$, $\zeta_{n,m}$ is the spectral-expansion coefficient of $\zeta(\lambda,\theta)$, and M means the largest total wavenumber in the model. The spectral coefficients are calculated through the spectral transform using the orthogonality of the spherical harmonics functions. For more details on the spherical harmonics spectral method, refer to Swarztrauber (1996), Galewsky et al. (2004), and Cheong (2006). The calculations were performed in double precision which provides 14 or 15 digits of decimal point for real variables. In spectral notation, the balanced field is expressed as

$$\Phi(\lambda,\theta) = \sum_{n=k}^{M}\sum_{k=0}^{M}\Phi_{n,k}P_n^k(\mu)\cos k\lambda , \quad (20)$$

where $\Phi_{n,k}$ is the spectral-expansion coefficient of $\Phi(\lambda,\theta)$. The coefficient $\Phi_{n,k}$ is obtained from the spectral coefficients of the nonlinear terms:

$$\Phi_{n,k} = -\frac{1}{n(n+1)}G_{n,k} - E_{n,k}, \quad (21)$$

where $G_{n,k}$ and $E_{n,k}$ are the spectral coefficients of G and $0.5(u^2+v^2)$, respectively.

The difference between analytic and numerical results is evaluated in terms of the l_2-norm on the spherical domain. The normalized difference of geopotential field is given by

$$l_2(\Phi) = \left[\sum_{i,j}\frac{(\Phi_{i,j}^A - \Phi_{i,j}^N)^2}{(\Phi_{i,j}^A)}\right]^{1/2}, \quad (22)$$

where the superscript A and N represent the analytical and numerical results, respectively, the summation is done over the globe, and the subscripts i and j denote the grid-point index. The number of transform Gaussian-grids is 320×160, which roughly corresponds to 1.875 resolution.

Fig. 2 presents the orthographic projection of the R-H wave of the first symmetric mode with zonal wavenumber 8 and the associated balanced field,

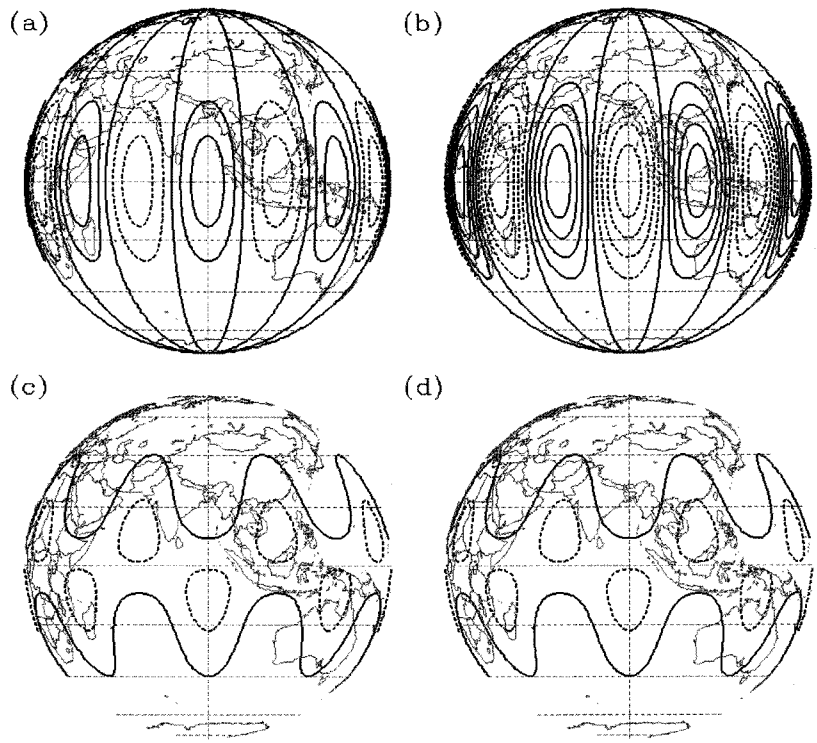

Fig. 2. The Rossby-Haurwitz wave of the first symmetric mode with zonal wavenumber 8 and the associated balanced field, which were illustrated with the orthographic map projection. (a) Streamfunction, (b) Vorticity, (c) Balanced geopotential obtained by analytical method, (d) Balanced geopotential calculated by spherical harmonics spectral method. The contour interval is 0.005 for (a), (c), and (d), and 0.2 for (b). Positive (negative) values are in solid (dashed) lines. The inclination of the rotation axis is zero ($\tau = 0$), the amplitude of the wave is $K = 0.013348$, and the background superrotation flow is not included ($\omega = 0$).

where $\tau = 0$, $K = 0.013348$, and $\omega = 0$ (see Eq. 18). The streamfunction and vorticity have a sectoral structure, where the perturbation of the same sign runs from the South pole to the North pole. It is noted that the geopotential fields in Fig. 2(c) and (d) exhibit the same structure over the globe, implying that the analytic formula was correctly derived. Althought the first antisymmetric mode for the geopotential field has only symmetric structure with respect to the equator (Phillips, 1959; Williamson and Browning, 1973; Williamson et al., 1992), the geopotential field in balance with the R-H wave of the first symmetric mode shows neither symmetric nor antisymmetric structure. When the balanced field is used as a validation method for a numerical model, this may be regarded as advantageous over the antisymmetric mode because it naturally provides a test bed for the performance of a model on maintaining the hemispheric symmetricity of the perturbation.

Fig. 3 is the same as Fig. 2 but for $\tau = \pi/3$, $K = 0.013348$, and $\omega = 1/70$. In this case, ω corresponds to $0.5\omega_s$ with ω_s being the strength of the mean flow which can make the R-H wave stationary. It is clear that a part of the wave pattern of geopotential is distorted to a large extent under the influence of the inclination of rotation axis, while the vorticity is little affected. This is due to large amplitude of the vorticity perturbation, compared to the zonal-mean part. Though not being clearly seen in this figure due to the orthographic projection, there is another distorted part of the geopotential field on the other longitudinal location (on the opposite side of the globe).

Table 1 presents $l_2(\Phi)$ for the case shown in Fig. 3 but for different inclination angles. The normalized

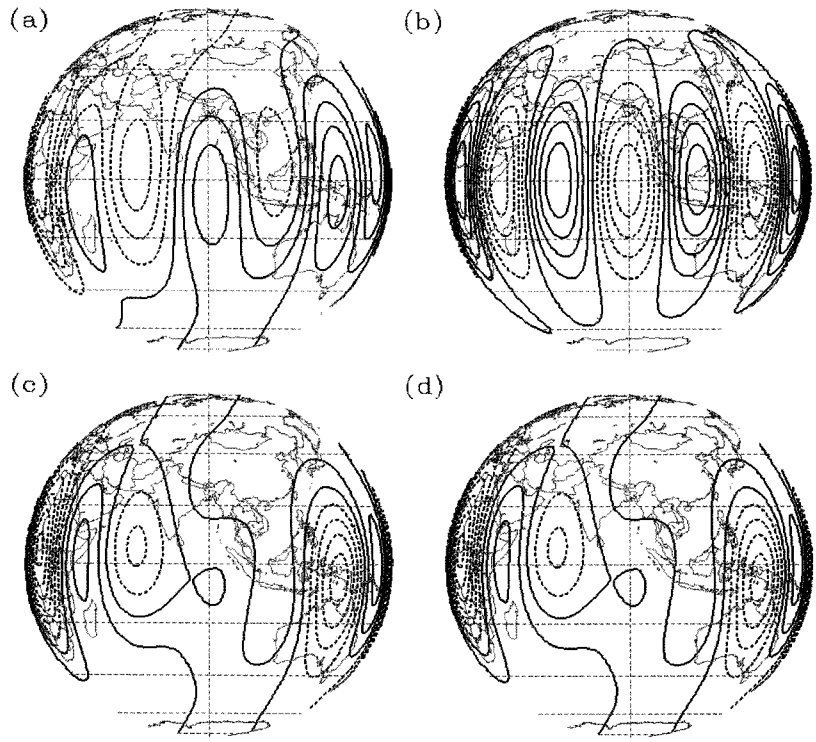

Fig. 3. The same as Fig. 2 except $\tau = \pi/3$ and $\omega = 1/70$.

differences in the order of machine rounding for all cases suggest that the analytic formula for the balanced geopotential is reliable. The normalized difference as shown in Table 1 does not seem to depend on the inclination angle of the rotation axis. The small variation of the difference within one order is not considered to be significant because they are near the machine rounding error.

Shown in Table 2 is the sensitivity of $l_2(\Phi)$ to the zonal wavenumber of the R-H wave m. It remains also in the order of machine rounding for all zonal wavenumber components. The normalized difference becomes larger for increased zonal wavenumber by about one order: It increased from about -15 to -14 where the zonal wavenumber changed from $m = 16$ to $m = 32$. The decreased accuracy for smaller scale is a common feature found in the calculation of the nonlinear differential equations with numerical method (Williamson et al., 1992; Thuburn and Li, 2000; Cheong, 2006). As long as the zonal wavenumber of the R-H wave is given much smaller than the truncation limit of the numerical model, the normalized difference is not likely to increase significantly.

Table 1. The inclination angle and the normalized difference between the analytical and calculated geopotential field for the Rossby-Haurwitz wave shown in Fig. 3

Inclination angle (τ)	$\log_{10} l_2$ (Φ)
$\pi/6$	-15.9780
$\pi/4$	-15.9970
$\pi/3$	-16.0666
$\pi/2$	-16.3254

Table 2. Dependence of the normalized difference between the analytical and calculated geopotential field for the Rossby-Haurwitz wave with $n = m$ on the zonal wavenumber. The dynamical parameters used are $K = 0.05$, $\tau = \pi/3$, and $\omega = [m(m+1) - 2]^{-1}$.

zonal wavenumber of Rossby-Haurwitz wave (τ)	$\log_{10} l_2$ (Φ)
4	-15.4598
8	-15.6809
16	-15.0260
32	-14.0961
48	-14.0683

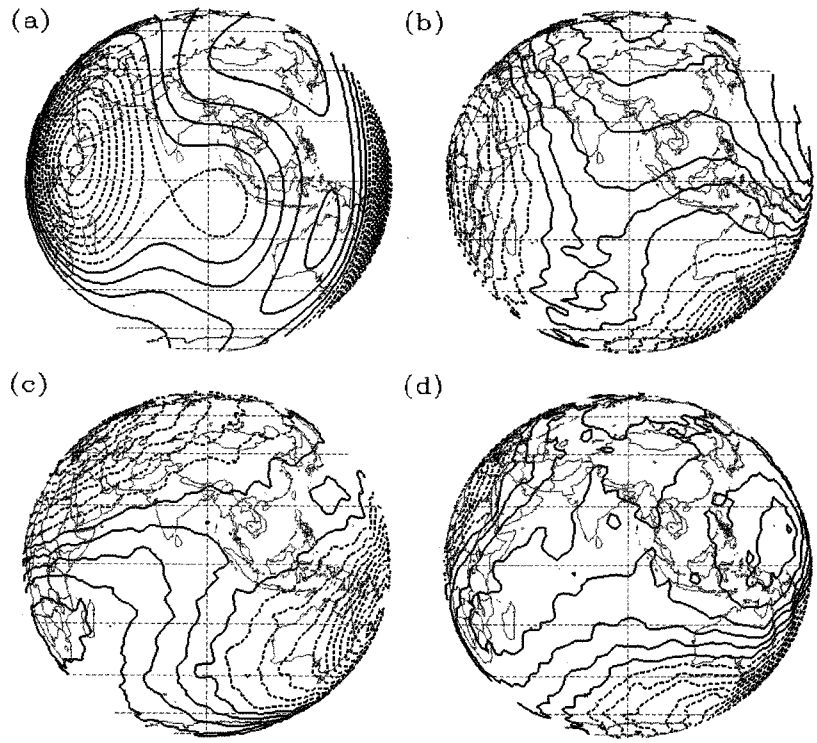

Fig. 4. The geopotential fields by day 0 (a), 15 (b), 30 (c), and 45 (d) which was obtained through the time integration of the shallow water spectral model with the initial condition of shallow-water Rossby-Haurwitz wave $(n,m)=(4,4)$. The amplitude of the wave and the strength of the superrotation background flow are $K=7.848\times10^{-6}\Omega^{-1}$ and $\omega=7.848\times10^{-6}\Omega^{-1}$ in nondimensional unit, respectively. Contour interval is 0.025, and positive (negative) values are in solid (dashed) lines.

The R-H wave is known to become unstable when the amplitude is sufficiently large (Baines, 1976; Hoskins, 1973; Thuburn and Li, 2000). In general, the stability decreases as the scale becomes smaller. Even the larger scale R-H wave has been proved to be unstable: For example, as shown by Thuburn and Li (2000) through numerical simulations using various models, the R-H wave $(n,m)=(5,4)$ which was used by authors (Phillips, 1959; Williamson et al., 1992; Cheong, 2006) was found to break down in case of long time integration. The R-H wave used in this study $(n=m)$ has a sectoral structure, i.e., there is no nodal point on meridian for the disturbance. This may be a favorable condition for the stability because the horizontal gradient of velocity for the sectoral mode is smaller than the tesseral mode if the zonal wavenumber is given the same.

To investigate the stability of the R-H wave and associated balanced field, the shallow water spectral model was time integrated for 50 days. The integration period of 50 days was found to be sufficient for this purpose (Thuburn and Li, 2000), because the amplitude of the unstable disturbance develops exponentially during the first 25 days and settles down to a nearly steady amplitude beyond that. For direct comparison with the results of Thuburn and Li (2000), the zonal wavenumber four was chosen, i.e., $(n,m)=(4,4)$. We can determine whether the wave is stable or not by inspecting the kinetic energy of the wave components other than zonal wavenumber four. However, to check the instability in more accurate way, it may be desirable to see the amplitude of the wave components which are related with the resonant triad (Baines, 1976): The wave components corresponding to the unstable resonant triad for $(n,m)=(4,4)$ is $(n,m)=(3,2)$ and $(n,m)=(6,2)$. In any case, if the R-

H wave of interest is unstable, the smooth initial field may appear in distorted structure for a long time-integration. Therefore, we decided to simply monitor the geopotential field to judge the instability.

Unlike the linear stability problem, we do not add artificial disturbance to the R-H wave because we are interested in the instability that grows from the numerical disturbance which has the order of machine rounding. As was proposed by Thuburn and Li (2000), a hyper diffusion of ∇^6 with the coefficient as can dissipate the smallest scale resolved in the model in 4 hours. The amplitude of the wave and the strength of the superrotation background mean flow are given the same as in Thuburn and Li (2000) to facilitate direct comparison.

The result of time integration is presented in Fig. 4, where the geopotential field by day 0, 15, 30, and 45 are illustrated. During time integration, the total kinetic energy remained almost in the constant value, indicating stable time integration without numerical overflow. As time elapses, the smooth geopotential field undergoes gradual change into a rather complicated structure which has evidently small scale disturbance embedded on the larger scale resembling the initial R-H wave. This clearly indicates that the initial wave was not broken down, i.e., the stability of the R-H wave. As was illustrated in Thuburn and Li (2000), when the R-H wave is unstable the large-scale feature is destroyed completely by the growing small-scale disturbances which originated from the machine rounding error.

Summary and Conclusions

In this study, the balanced geopotential field associated with the sectoral R-H waves was presented in analytical approach. The balanced field was obtained by inverting the nonlinear divergence equation with the time derivative being zero. The geopotential field was found to be asymmetric with respect to the equator, and it was expressed with six zonal wavenumber components in the presence of the inclination of the rotation axis. Comparison of the analytical geopotential with that obtained by the spherical harmonics spectral model showed a good agreement between them with the normalized difference whose order is close to the machine rounding. The stability of the balanced field associated with the sectoral mode of the R-H wave was investigated in terms of the long-term time integration using the spherical harmonics spectral model. From the geopotential field which has maintained the large-scale initial structure with small-scale disturbances imbedded on it, the wave was found to be stable. The results of the study indicate that the sectoral R-H wave and the balanced field associated with it is more useful than the first antisymmetric mode to validate a numerical model in that they are more stable and of sasymmetric structure about the equator.

Acknowledgments

This work was supported by PuKyong National University Research Foundation Grant in 2005 PR-2005-007. The computations were performed on IBM supercomputer under the grand challenge support program 2007 of Supercomputing Center in the Korea Institute of Science and Technology Information (KISTI). The authors wish to thank the anonymous reviewers for useful comments.

References

Baines, P.G., 1976, The stability of planetary waves on a sphere. J. Fluid Mech., 73, 193-213.

Browning, G.L., Hack, J.J., and Swarztrauber, P.N., 1989, A comparison of three numerical methods for solving differential equations on the sphere. Mon. Wea. Rev., 117, 1058-1075.

Cheong, H.-B., 2006, A dynamical core with double Fourier series: Comparison with the spherical harmonics method. Mon. Wea. Rev., 134, 1299-1315.

Daley, R., 1983, Linear non-divergent mass-wind laws on the sphere. Tellus, 35A, 17-27.

Galewsky, J., Scott, R.K., and Polvani, L.M., 2004, An initial-value problem for testing numerical models of the shallow water equations. Tellus, 56A, 429-440.

Haurwitz, B., 1940, The motion of atmospheric disturbances on the spherical earth. J. Mar. Res., 3, 254-267.

Hoskins, B.J., 1973, Stability of the Rossby-Haurwitz wave. Quart. J. Roy. Meteorol. Soc., 99, 723-745.

Läuter, M., Handorf, D., and Dethloff, K., 2005, Unsteady analytical solutions of the spherical shallow water equations. J. Comput. Phys., 210, 535-553.

Orszag, S.A., 1970, Transform method for calculation of vector coupled sums: Application to the spectral form of the vorticity equation. J. Atmos. Sci., 27, 890-895.

Ortland, D.A., 2005, Generalized Hough mode: The structure of damped global-scale waves propagating on a mean flow with horizontal and vertical shear. J. Atmos. Sci., 62, 2674-2683.

Phillips, N.A., 1959, Numerical integration of the primitive equations on the hemisphere. Mon. Wea. Rev., 87, 333-345.

Swarztrauber, P.N., 1996, Spectral transform methods for solving the shallow-water equations on the sphere. Mon. Wea. Rev., 134, 730-744.

Thuburn, J. and Li, Y., 2000, Numerical Simulations of Rossby-Haurwitz waves. Tellus, 52, 180-189.

Williamson, D.L. and Browning, G.L., 1973, Comparison of grids and difference approximations for numerical weather prediction over the sphere. J. Appl. Meteor., 12, 264-274.

Williamson, D.L., Drake, J.B., Hack, J.J., Jakob, R., and Swarztrauber, P.N., 1992, A standard test set for numerical approximations to the shallow water equations in spherical geometry. J. Comput. Phys., 102, 211-224.

2007년 8월 22일 접수
2007년 11월 5일 수정원고 접수
2007년 11월 28일 채택